New Kinetics of $CaCO_3$ Nucleation and Microgravity Effect

X. Y. Liu,*,† K. Tsukamoto,‡ and M. Sorai‡

Department of Physics, The National University of Singapore, 10 Kent Ridge Crescent, Singapore, and Faculty of Science, Tohoku University, Aramaki Aoba, Sendai 980-8578, Japan

Received September 17, 1999. In Final Form: March 6, 2000

Many organic and inorganic substrates or particles play a crucial role in mediating crystallization by providing effective nucleation sites[1] for crystals. The occurrence of these particles not only establishes the crystallization process but also has a significant impact on the size, pattern formation, and hardness of the materials. An understanding of the effect of these substrates or particles on the nucleation process opens up new and promising routes for achieving a controlled synthesis of complex crystalline structures, applicable across a broad spectrum of materials-based technologies, and has also significant implications for life sciences. Because $CaCO_3$ occurs abundantly in industrial crystallization and biomineralizing systems[2] and crystallized easily, it has emerged as a model crystal[3−5] for developing this understanding.[2,6−8] We notice that although much work on $CaCO_3$ nucleation has already been carried out,[9] a genuine understanding has not been obtained yet.

Here we will examine the nucleation kinetics of $CaCO_3$ from solution using a newly developed advanced fast dynamic light scattering method (FDLS).[10,1110,11] This new method enables us to measure the sizes and size distribution of the nuclei, with radii ranging from a few nanometers to a few tens of micrometers, at successive time intervals of a few seconds. Thus the present technique is 10 times faster than conventional dynamic light scattering (DLS) measuring techniques. This allows an in situ measurement of the nucleation and the size increase of the nuclei. To obtain a comprehensive and fundamental understanding, the experiments were carried out under both gravity and microgravity.

In the experiments, the ionic strength is fixed at 0.11 M. The experiments were carried out in a stopped-flow system, and the rate of $CaCO_3$ nucleation was measured by FDLS (see Figure 1).[10,11] The two solutions were filtered with filters of a pour diameter of 0.2 μm prior to the experimental runs. A summary for the experimental setup and conditions is given in Table 1. It shows that the conditions for both the gravity and microgravity experiments are (nearly) the same.

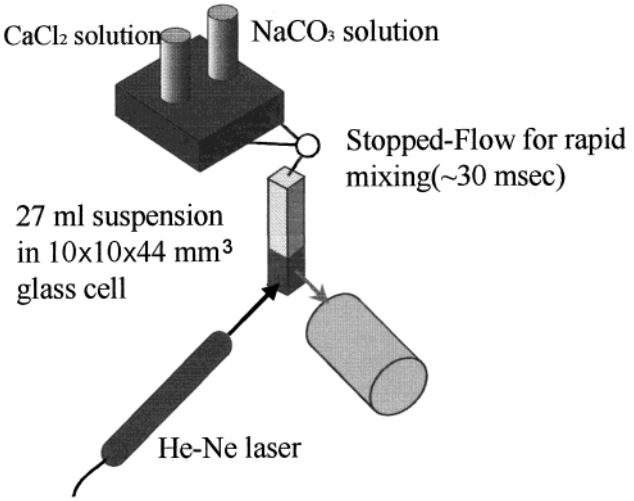

Figure 1. Schematic illustration of experimental setup of FDLS for the measurement of the incubation time of nucleation.

Table 1. Summary of Experimental Setup and Conditions

	exptl setup	temp, T (K)	pressure, P (atm)	pH
microgravity	FDLS	~297	0.95	10.3−11.3
gravity	FDLS	~300	1	10.3−11.3

In the beginning the $CaCl_2$ and Na_2CO_3 solutions were mixed and introduced to a rectangular glass cell (10 × 10 × 44 mm^3) via a stopped-flow system. The system allows homogeneous mixing of the two solutions within about 20 ms. The measurement of the incubation time τ started immediately after the two solutions were mixed. This allowed sufficient time for rapid measurement. Good reproducibility was obtained by using this experimental setup.[10,11]

For the microgravity experiments, a MU-300 double-jet airplane was used to attain a microgravity duration of 20 s during a parabolic flight. Although such a time scale is too short for the measurement of the incubation time of nucleation using conventional DLS, it is nevertheless sufficient for measuring τ using FDLS. In our experiments, the solution concentration was adjusted so that the nucleation could be obtained in less than 20 s.

The supersaturation σ is defined according to thermodynamics, by[12]

$$\ln(1+\sigma) = \Delta\mu/kT \quad (1a)$$

$$= \ln(a/a_e) \quad (1b)$$

and for a $CaCO_3$ solution

$$\ln(1+\sigma) = \ln[a(Ca^{2+})a(CO_3^{2-})/K_{sp}] \quad (2)$$

where $\Delta\mu$ denotes the chemical potential difference between the actual state and the equilibrium state under a given condition, k is the Boltzmann constant, T is the

† The National University of Singapore.
‡ Tohoku University.

(1) Winter, A.; Seisser, S. G. *Coccolithophores*; Cambridge University Press: New York, 1994.
(2) Belcher, A. M.; Wu, X. H.; Christensen, R. J.; Hansma, P. K. *Nature* **1996**, *381*, 56.
(3) Berman, A.; Addadi, l.; Weiner, S. *Nature* **1988**, *331*, 546.
(4) Mann, S.; et al. *Science* **1993**, 261, 1286.
(5) Mann, S. *Nature* **1993**, *365*, 499.
(6) Teng, H. H.; Dove, P. M. *Am. Mineral.* **1997**, *82*, 878.
(7) Walters, D. A.; et al. *Biophys. J.* **1997**, *72*, 1425.
(8) Sikes, C. S.; Yeung, M. L.; Wheeler, A. P. In *Surface Reactive Peptides and Polymers*: *Discovery and Commercialization*; Sikes, C. S., Wheeler, A. P., Eds.; American Chemical Society: Washington, DC, 1991; pp 50−71.
(9) Söhnel, O.; Mullin, J. W. *J. Cryst. Growth* **1998**, *44*, 377−382.
(10) Tsukamoto, K. *Extended Abstract of AIST Workshop*, Sapporo, Oct. 1998; pp 29−33.
(11) Tsukamoto, K.; Maruyama, S.; Shimizu, K.; Kawasaki, H.; Morita, T. S. *Reports of Microgravity Experiments by Aircraft* **1998**, *7*, 51−57.
(12) Chernov, A. A. *Modern Crystallography III−Crystal Growth*; Springer-Verlag: Berlin, 1984.

10.1021/la9912287 CCC: $19.00
Published on Web 05/16/2000

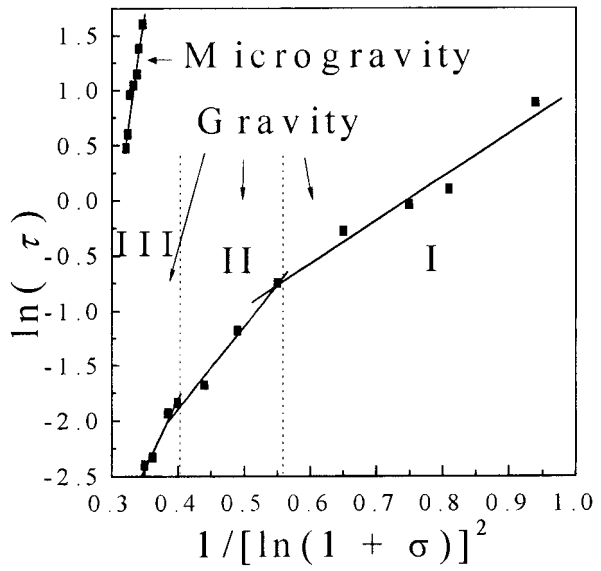

Figure 2. ln τ vs $1/[\ln(1+\sigma)]^2$ is plotted for the nucleation of $CaCO_3$ in gravity and microgravity. In gravity, three straight lines of different slops intercept with each other, dividing the space into three regimes. Under gravity, the slope is four times larger than the the slope of a similar experiment obtained from the gravity experiments. The experimental error for the measurements of τ is about 0.2 in the ln scale.

absolute temperature, a and a_e are the actual and equilibrium activities, respectively, K_{sp} is the equilibrium solubility at zero ionic strength, and $a(i)$ is the activity of species i.

It has to be noticed that there are some standing issues associated with previous knowledge on nucleation. As the first, the nucleation rate is given according to classical nucleation theories as[12−14]

$$J = B \exp\left[-\frac{l\Delta G^*_{\text{homo}}}{kT}\right] \tag{3}$$

with

$$\Delta G^*_{\text{homo}} = \frac{16\pi}{3}\frac{\Omega^2 \gamma_{\text{cf}}{}^3}{\Delta\mu^2} \tag{4}$$

where B is the kinetic constant, γ_{cf} denotes the specific interfacial free energy between the crystals and the mother phase, Ω is the volume of growth units, and l ($0 \le l \le 1$) is a factor describing the reduction of the nucleation barrier due to a foreign body.[15,1615,16] Equation 3 gives the nucleation rate: the case of homogeneous nucleation corresponds to $l = 1$, whereas heterogeneous nucleation corresponds to $l < 1$. According to eq 3, the rate of homogeneous nucleation is considered to be always lower than that of heterogeneous nucleation.

As the second point, it is believed[13−16] that at low supersaturations heterogeneous nucleation will be dominant, whereas at high supersaturations homogeneous nucleation will occur. However, this is not well described by eqs 3 and 4.

Nucleation kinetics is often examined by measuring the incubation time of nucleation τ. Considering that τ is proportional to $1/J$, and adopting eq 3 to describe the nucleation kinetics, we have then

$$\ln \tau = \frac{16\pi}{3}\frac{\Omega^2(\gamma_{\text{cf}}/kT)^3 l}{[\ln(1+\sigma)]^2} - \ln B \tag{5}$$

According to eq 5, the line representing heterogeneous nucleation ($l < 1$) lies always below that of homogeneous nucleation ($l = 1$). As regards the second consideration above, the lines of homogeneous and heterogeneous nucleation will intercept at a certain supersaturation σ^*. At $\sigma < \sigma^*$, the line of heterogeneous nucleation lies below that of homogeneous nucleation while at $\sigma > \sigma^*$ the line of homogeneous nucleation lies below that of heterogeneous nucleation.

For the aforementioned system, under gravity, the supersaturation σ varies between 5.7 and 1.7. A plot of ln τ as a function of $1/[\ln(1+\sigma)]^2$ is given in Figure 2. It is surprising to see that within the range of supersaturations, three straight lines of different slopes intersect pairwise, partitioning the space into three regimes. The slopes of the three lines are summarized in Table 2. The results of Figure 2 and Table 2 indicate that *nucleation is controlled by at least three different nucleation processes in different regimes*.

For microgravity, a straight line was obtained in regime III under a similar condition (see in Table 1), which gives a slope of 42. Amazingly, this result is almost four times larger than the value obtained in gravity within a comparable supersaturation regime (cf. Table 2 and Figure 2). According to eq 3, this should simply mean that *the "measured interfacial tension" of $CaCO_3$ in gravity is 1.6 time "lower" than that in microgravity*. Obviously, this condition is logically unacceptable.

Evidently, our previous knowledge of nucleation is inadequate for interpreting both the gravity and the microgravity results. A new understanding should be developed to capture the nucleation kinetics of $CaCO_3$. In the following we will apply a newly developed kinetic model[17] to examine the nucleation of $CaCO_3$ under both gravity and microgravity conditions.

Accordingly, the nucleation rate is given by

$$J = 4\pi a(R^s)^2 N^o l''(m,R')[l(m,R')]^{1/2} B \times \exp\left[-\frac{16\pi\gamma_{\text{cf}}{}^3\Omega^2}{3kT[kT\ln(1+\sigma)]^2}\, l(m,R')\right] \tag{6}$$

with

$$B = (n_1)^2 4\alpha\beta_{\text{sl}}'\Omega\left(\frac{\gamma_{\text{cf}}}{kT}\right)^{1/2} \tag{7}$$

$$l''(m,R') = \frac{1+(1-R'm)/q}{2} \tag{8}$$

$$l(m,R') = \frac{1}{2} + \frac{1}{2}\left(\frac{1-mR'}{q}\right)^3 + \frac{1}{2}(R')^3\left[2 - 3\left(\frac{R'-m}{q}\right) + \left(\frac{R'-m}{q}\right)^3\right] + \frac{3}{2}m(R')^2\left(\frac{R'-m}{q} - 1\right) \tag{9}$$

$$q = [1 + (R')^2 - 2(R')m]^{1/2} \tag{10}$$

$$R' = R^s/r_c \tag{11}$$

and the critical size of the nuclei is

$$r_c = 2\Omega\gamma_{\text{cf}}/\Delta\mu \tag{12}$$

($1 \le l(m,R') \le 0$). (The details of the derivation for eq 6 will be published elsewhere.[17]) In eqs 6−9, m depends on the interaction between the crystalline phase and the nucleating particles and is expressed as a function of

Table 2.

supersaturation regime	gravity: regime I ($\sigma \approx 1.7-2.8$)	gravity: regime II ($\sigma \approx 2.8-3.8$)	gravity: regime III ($\sigma \approx 3.8-5.2$)	microgravity: $\sigma \approx 3.8-5.2$ (regime III)
slope [$\kappa l(m,R')$]	3.9	7.5	12.5	42.0

interfacial free energies between different phases

$$m = (\gamma_{sf} - \gamma_{sc})/\gamma_{cf} = \cos\theta \qquad (13)$$

(γ_{sf}, γ_{sc}, and γ_{cf} correspond to the interfacial tension between substrate and fluid, crystal and substrate, and crystal and fluid, respectively.)

Energetically, similar to the previous quantity l, $l(m,R')$ in the exponential term describes the reduction of the nucleation barrier from a genuine homogeneous nucleation ΔG^*_{homo} to the actual heterogeneous nucleation ΔG^*, due to the presence of foreign bodies. In Figure 3a, $l(m,R')$ is shown as a function of m and R'. When $R' \rightarrow 0$ or $m = -1$, $l(m,R') = 1$, corresponding to the situation where the size of substrate is very small in comparison with the critical nuclei or the interactions and structural match between the nuclei and the substrates are very poor. This is equivalent to the case of homogeneous nucleation. The case that $m \rightarrow 1$, $l(m,R') = 0$ represents perfect interactions and structural matching between nuclei and substrates. In the latter case, foreign particles reduce to seed crystals. It follows from Figure 3a that when $R' \geq 1$, $l(m,R')$ or ΔG^* vanish completely. This extreme case corresponds to growth. Normally heterogeneous nucleation occurs in the range of m between 1 and -1, or $l(m,R')$ between 0 and 1, depending on the nature of the substrate surface and on supersaturation. In the case of $R' \gg 1$, a small nucleating particle reduces to a planar substrate. Then expression 1 describes the nucleation on a plane surface. $l''(m,R')$ gives a similar plot as given by Figure 3a.

We notice that in the case of homogeneous nucleation, one has $l'(m,R') = l(m,R') = 1$, and $4\pi a(R^s)^2 N^o \rightarrow 1$. Then, eq 6 is reduced to eq 5.

Kinetically, both $l(m,R')$ and $l''(m,R')$ generally describe the major difference between homogeneous and heterogeneous nucleation kinetics as indicated by eq 6. On one hand, the occurrence of foreign particles will lower the nucleation barrier, resulting in an increase in the nucleation rate. As mentioned before, this effect, described by $l(m,R')$, will be enhanced by increasing the interaction between the crystal phase and the substrate and/or with the relative size of the foreign particles R'. On the other hand, nucleation on foreign bodies exerts also a negative impact on the kinetics. As shown in Figure 3b, nucleation on a foreign particle will reduce the "effective surface" of collision of embryos, where growth units are incorporated into embryos. This tends to slow the nucleation kinetics, contrary to the effect of lowering the nucleation barrier. This negative effect is mainly described by $l''(m,R')$ and $l(m,R')$ in the pre-exponential term of J given by eq 6.

In terms of the nucleation kinetics, these factors will play different roles in different regimes. At low supersaturations, the nucleation barrier is very high. The top priority in accelerating the kinetics is to lower the nucleation barrier. Then the occurrence of heterogeneous nucleation with a low $l(m,R')$ will be kinetically favored. Conversely, at higher supersaturations, the exponential term associated with the nucleation barrier becomes less important. Instead, the issue of effective collisions, described by the pre-exponential factors $l(m,R')$ and $l''(m,R')$, becomes more dominant. It follows that nucle-

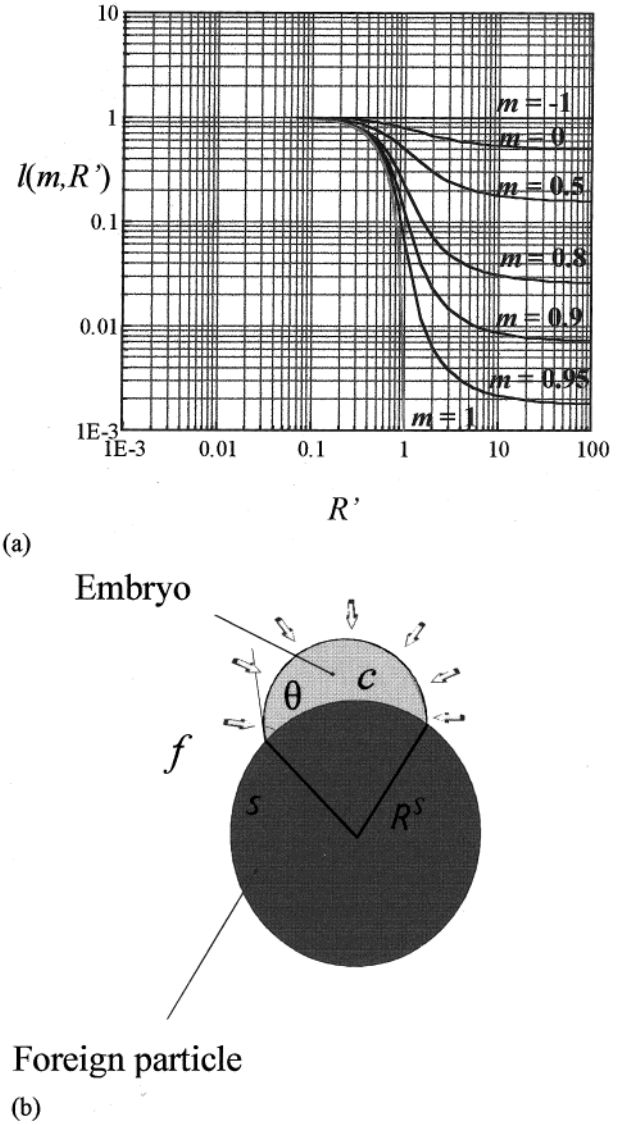

Figure 3. (a) Dependence of factor $l(m,R')$ on the relative particle size $R' = R^s/r_c$ and m. $R' \rightarrow 0$ implies that foreign particles as the nucleating substrate vanish completely. $m = -1$ corresponds to the case where foreign particles and embryos are repulsive to each other. This corresponds to the situation where foreign particles do not catalyze the nucleation any more. With increasing R' ($R' \geq 0.01$) and/or m ($-1 \leq m \leq 1$), $l(m,R')$ decreases correspondingly. Referring to eq 1, this implies that the nucleation barrier ΔG^* is ranging from ΔG^*_{homo} to 0 ($0 \leq \Delta G^* \leq \Delta G^*_{homo}$). In this regime, foreign particles play a crucial role in lowering the nucleation barrier. (b) Schematic illustration of heterogeneous 3D nucleation on a foreign particle with a radius of R^s and interaction parameter m. Embryo, "c"; nucleating particle, "s"; mother phase, "f".

(13) Nielsen, A. E.; Christofferesen, J. In *Biological Mineralisation and Demineralisation*; Nancolllas, G. H., Konferenzen, D., Eds.; Springer-Verlag: Berlin, 1982; pp 37−77.
(14) Skripov, V. P. In *Current Topics In Materials Science*; Kaldis, E., Scheel, H. J., Eds.; North-Holland: Amsterdam, 1977; Vol. 2, pp 327−378
(15) Chayen, N. E. *J. Appl. Crystallogr.* **1997**, *30*, 108−203.
(16) Malkin, A. I.; Chernov, A. A.; Alexeev, I. V. *J. Cryst. Growth* **1989**, *97*, 765.
(17) Liu, X. Y. *J. Chem. Phys.* **1999**, *111*, 1628−1635.

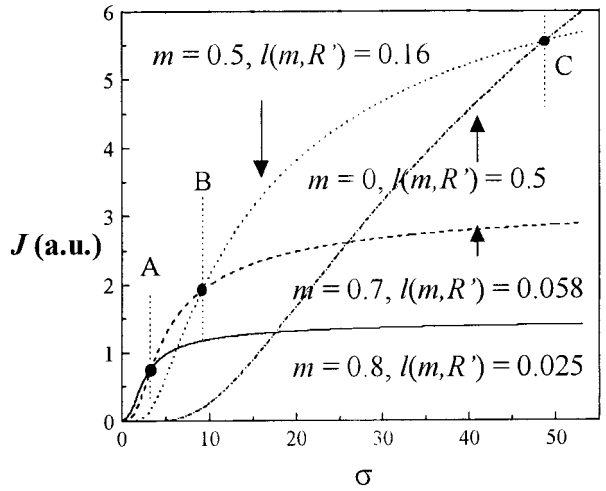

Figure 4. Dependence of the relative nucleation rate on the supersaturation. The effect of m (or contact angle θ between foreign particles and the nucleating phase) on the nucleation rate. As shown, foreign particles with a large m (or a small $l(m,R')$) will control the kinetics at low supersaturations while those with a small m (or a large $l(m,R')$) will control the kinetics at high supersaturations. $R^s = 1000a$, $\gamma_{cf}\Omega^{2/3}/kT = 1.5$ (a is the demension of growth units.)

ation on substrates having a larger $l(m,R')$ and $l''(m,R')$ becomes kinetically more favorable.

In Figure 4, the nucleation rate J (in arbitary units) is plotted versus the relative supersaturation σ according to eq 6 for different values of m for the foreign particles. As expected, nucleation on foreign particles with small $l(m,R')$ and $l''(m,R')$ (a large m and/or a large radius) is dominant at low supersaturations, whereas nucleation on those with large $l(m,R')$ and $l''(m,R')$ (a lower m and/or a small radius) governs the kinetics at high supersaturations. This implies that for a given system, different foreign particles having distinct surface properties and/or different sizes will control nucleation in different supersaturation regimes. Homogeneous nucleation can be regarded as an upper limiting case of heterogeneous nucleation where one has $l(m,R') = l''(m,R') = 1$. As shown in Figure 4, theoretically this happens under normal conditions only at very high supersaturations.

The evidence for the above analytical results can be identified from the plot of $\ln \tau$ vs $1/[\ln(1+\sigma)]^2$. The slope of the straight line is given by $\kappa l(m,R')$ ($\kappa = 16\gamma_{cf}^3\Omega^2/3(kT)^3$ is a constant for a given system). The change of $l(m,R')$ at different supersaturations is directly responsible for the change of the slope. In other words, the slope corresponds to the relative $l(m,R')$. As shown by Figure 2, under gravity, the three intersecting straight lines with different slopes indicate that the nucleation is controlled by three different types of foreign bodies within the corresponding regimes. Considering that supersaturation increases progressively from regime I to III, if we denoted $l(m,R')$ in these three regions as $[l(m,R')]_I$, $[l(m,R')]_{II}$, $[l(m,R')]_{III}$, respectively, we should have then $[l(m,R')]_I < [l(m,R')]_{II} < [l(m,R')]_{III}$. This is in excellent agreement with the values given in Table 2.

The microgravity effect on nucleation can be understood in terms of convection. Under gravity, convection due to temperature or concentration gradient caused by nucleation and growth helps the transport of growth units to the surface of substrates. This will compensate for the concentration (or supersaturation) depression during nucleation. It will also help to bring new seed crystals from the substrate surface to the bulk. This virtually enhances the "number" of effective foreign bodies for heterogeneous nucleation. In general, convection will substantially promote the effect of foreign bodies, such as tiny particles and organic species on the wall of the crystallization vessels, which inevitably occur in all crystallization systems. Once heterogeneous nucleation occurs at relatively low supersaturations, nucleating materials are consumed quickly. This leads then to a drop in the bulk supersaturation. Therefore, the supersaturation required for genuine homogeneous nucleation becomes extremely difficult to reach.

Under microgravity, the convection attributed to gravity is suppressed. The upstream convection plume caused by gravity will lead to an inhomogeneity in the scattering image, which can be detected by the video−microscopic imaging system. It was shown in our experiments that gravitational sinks due to the convection of the solution are very prominent in gravity and have an average size of 600 nm in diameter. The gravitational sinks disappear soon after microgravity is introduced. Therefore, the image obtained in microgravity is much more uniform than that obtained in normal gravity. This indicates that the convection due to the concentration and temperature gradient is eliminated in microgravity. As a consequence, microgravity will significantly slow the transport of growth units toward the substrate surface, causing the concentration (or supersaturation) depression during nucleation on the surface of substrates. This implies that a much larger supersaturation is needed in order to achieve a similar nucleation rate for heterogeneous nucleation. Taking $l(m,R') = 1$, the interfacial free energy obtained from the microgravity experiments (cf. eq 4) is 170 mJ/m^2 at 25 °C, almost the same as that obtained from the contact angle measurements.[18] This result strongly suggests the occurrence of homogeneous nucleation in microgravity. Therefore, *in microgravity, heterogeneous nucleation is suppressed to a larger extent so that homogeneous nucleation may be achieved more easily.*

(18) Tsukamoto, K. To be submitted for publication.

LA9912287